

2004 年釧路沖地震及び根室沖想定地震に関する研究

Research on the 2004 Kushiro-oki earthquake and the future
Nemuro-oki earthquake

Index

1. Proposes of the Project
 2. The 2004 Kushiro-oki Earthquake
 - 2.1 Introduction
 - 2.2 Seismological Analysis
 - 2.2.1 Teleseismic Waveform Analysis
 - 2.2.1.1. Point Source Solution
 - 2.2.1.2. Source Process
 - 2.2.2. Aftershock Sequence
 - 2.2.2.1. Data
 - 2.2.2.2. Relocation of Hypocenters
 - 2.2.2.3. Location Errors
 - 2.2.2.4. Results
 - 2.2.3. Source Process and Aftershock Distribution
 - 2.3. Tsunami Analysis
 - 2.3.1. Data
 - 2.3.2. Analysis
 - 2.3.3. Results
 - 2.4. Discussions
 - 2.4.1. Source Process and Aftershock Distribution
 - 2.4.2. Average Stress Drop
 - 2.4.3. Seismic Quiescence Area and the Asperity Ruptured by the 1973 Nemuro-Oki Earthquake
 - 2.5. Concluding Remarks
 3. A future Nemuro-Oki earthquake
 - 3.1. Introduction
 - 3.2. The 1973 and 1894 Nemuro-Oki earthquake
 - 3.2.1. Data and Method
 - 3.2.2. Results
 - 3.3. The Seismic Activity Using Ocean Bottom Seismic Network
 - 3.3.1. Data
 - 3.3.2. Results
 - 3.4. Discussions
- References
- Published paper

1. Proposes of the Project

On November 29, 2004, a large earthquake (M_{jma} 7.1) occurred off Kushiro. The earthquake has been expected by the Headquarters for Earthquake Research Promotion in Japan (HERP) before the earthquake occurred. The probability of the occurrence of the earthquake during 30 years from October 1, 2003, was estimated to be about 80 % according to the HERP. The 2003 great Tokachi earthquake occurred in the west of the 2004 Kushiro earthquake has been also expected by the HERP before the earthquake occurred. Furthermore, A future great Nemuro-oki earthquake has been also expected by the HERP with the high probability of the occurrence during 30 years from October 1, 2003, 20-30%. If the future Nemuro-oki earthquake occur, it is possible to cause large damages near the source area in Hokkaido.

In this research project, we first try to understand the source process of the 2004 Kushiro-oki earthquake, using the seismological and tsunami analyses. Next, for the future Nemuro-oki earthquake, the earthquake activity along the plate interface near the source region is studied using the ocean bottom seismogram network. Also, the tsunami analysis of the 1894 Nemuro-oki earthquake is carried out to discuss the size of the future earthquake.

2. The 2004 Kushiro-oki Earthquake

2.1 Introduction

At 3:32 on 29 November 2004 in Japan Standard Time, a large earthquake occurred off the coast of Kushiro (or Shiranuka) in the eastern Hokkaido, Japan (Fig. 1). Japan Meteorological Agency (JMA) determined the epicenter = (42.944°N, 145.280°E), the depth = 48.2 km, and the magnitude (M) = 7.1. Many aftershocks followed the main shock including two events larger than $M = 6.0$: $M = 6.9$ on 6 December 2004 and $M = 6.4$ on 18 January 2005. This sequence of the main shock and aftershocks should be noteworthy since the focal area was located between the asperity ruptured by the 1973 Nemuro-Oki earthquake (Yamanaka and Kikuchi, 2002) and the on-going seismic quiescence area (Katsumata and Kasahara, 2004). In the Nemuro-Oki area, Katsumata and Kasahara (2004) found that the microearthquake seismicity rate within the Pacific plate decreased 48 %, which started in June 2000 and has been lasting approximately five years. The seismic quiescence area is defined by a circle centered at (43.4°N, 145.0°E) with a radius of 46 km.

Before the 1973 Nemuro-Oki earthquake, the Tokachi-Oki earthquake ($M = 8.1$) occurred in 1952, and the Kushiro-Oki earthquake ($M = 7.2$) occurred in August 1961 that was followed by the largest aftershock ($M = 6.9$) in November 1961. While on the other hand the Tokachi-Oki earthquake ($M = 8.0$) occurred in 2003, which ruptured the same asperity as that of the 1952 Tokachi-Oki earthquake (Yamanaka and Kikuchi, 2003), and the Kushiro-Oki earthquake ($M = 7.1$) occurred in November 2004, which was followed by the largest aftershock ($M = 6.9$) in December 2004. The sequence of these events is very similar to that after the 1952 Tokachi-Oki earthquake.

The purpose of this session is to describe the 2004 Kushiro-Oki earthquake sequence in detail by determining the source process of the main shock using teleseismic body waves or tsunami waveforms and relocating aftershocks.

2.2 Seismological Analysis

2.2.1 Teleseismic Waveform Analysis

2.2.1.1. Point Source Solution

We retrieved the broad-band seismograms archived by Data Management Center of IRIS (Incorporated Research Institutions for Seismology) and chose the stations at epicentral distances between 30° and 100° for the P wave, and the stations between 30° and 50° for the SH wave, as shown in Fig. 2. The azimuthal coverage is good. We selected sixteen vertical components of P wave data and two SH wave data. All the records were converted into ground motion displacement with a sampling rate of 1 Hz, and band-pass filtered between 0.004 and 1 Hz.

Before estimating a space-time distribution of slip, we determined the focal mechanism and the depth of hypocenter for a single point source by using the method developed by Kikuchi and Kanamori (1991). Synthetic waveforms were calculated on the assumption that a near-source structure consisted of three layers as shown in Table 1, which is based on Iwasaki et al. (1989). We modeled a source time function by an isosceles triangle with duration of 8 sec.

We found that the calculated waveforms fitted the observations best if we assumed that the depth of hypocenter was 50 km and the focal mechanism was a reverse faulting on a shallow dipping plane: (strike, dip, slip) equal to $(238^\circ, 33^\circ, 117^\circ)$, rather than a steep dipping plane: $(27^\circ, 61^\circ, 74^\circ)$ (Fig. 3a). This result is consistent with solutions obtained by USGS, $(239^\circ, 29^\circ, 120^\circ)$, and by Harvard University, $(242^\circ, 26^\circ, 122^\circ)$.

2.2.1.2 Source Process

By careful inspection of recorded waveforms, a phase due to the main rupture was clearly identified several seconds after the arrival time of the P wave. We modeled this

phase with a waveform inversion method developed by Kikuchi and Kanamori (2003). We assumed a planar fault with a strike of 238° and a dip of 33° , which are same as those obtained in the previous section, and the area of $35 \times 30 \text{ km}^2$. The fault plane was divided into 7×6 subfaults with an area of $5 \times 5 \text{ km}^2$. Point sources placed at the center of each subfault for calculating synthetic waveforms. At all the point sources, the strike and the dip were fixed to be 238° and 33° , respectively, and the moment rate function and the slip direction were unknown parameters in the inversion.

We investigated the depth of the initial break point by a grid search method varying the depth by 1 km, and found that the best solution was obtained at a depth of 48 km. This depth corresponds to the upper boundary of the seismic plane associated with the subducting Pacific plate (Katsumata et al, 2003). We also investigated the rupture velocity by a grid search method, and found that it is 3.0 km/s.

Fig. 3b shows a time history of a moment rate, dM_0/dt , and Fig. 4 shows the observed and the synthetic waveforms for the 29 November 2004 $M7.1$ Kushiro-Oki earthquake. The rupture duration time, that is, the rise time plus the rupture propagation time, was 10 sec. The total seismic moment was $M_0 = 3.4 \times 10^{19} \text{ Nm}$, that is, $M_w = 7.0$, which is consistent with the CMT solutions obtained by USGS, $M_0 = 3.7 \times 10^{19} \text{ Nm}$, and by the Harvard University, $M_0 = 3.65 \times 10^{19} \text{ Nm}$. Fig. 3c shows a slip distribution on the assumed fault plane. At each grid point, we calculated the displacement, D , from the seismic moment, m_0 , obtained by the waveform inversion, the area $A = 5 \times 5 \text{ km}^2$, and the rigidity $\mu = 60 \text{ GPa}$, using an equation, $m_0 = \mu DA$. A large displacement is located around the initial break point, suggesting that the rupture propagated concentrically. The displacement was largest, amounting to 3.1 m, at a grid of the initial break point.

The final source parameters of the 29 November 2004 Kushiro-Oki earthquake are summarized as follows: the total seismic moment $M_0 = 3.4 \times 10^{19} \text{ Nm}$, that is, $M_w = 7.0$; (strike, dip, slip) = (238, 33, 117); depth of the initial break point = 48 km; source duration time = 10 sec; and the maximum displacement = 3.1 m.

2.2.2. Aftershock Sequence

2.2.2.1. Data

We used two data sets of arrival times of P and S waves, and relocated aftershocks. One was based on readings of the arrival times produced by a daily routine work at Institute of Seismology and Volcanology, Hokkaido University (ISV) (Data set 1), and another one was produced by the authors for ourselves (Data set 2).

Data set 1.

Seismographic stations that ISV used for hypocenter location are shown in Fig. 5a.

Katsumata et al. (1995) and Katsumata et al. (2003) described on the daily routine work at ISV. From the seismic catalog compiled by ISV between 1 January 2002 and 29 January 2005, we selected earthquakes which filled the following six criteria: (1) error ellipse smaller than 1 km in the North-South and the East-West directions and 2 km in the depth direction, (2) root mean square (rms) of the residuals of P wave less than 0.5 s, (3) rms of the residual of S wave less than 1.0 s, (4) readings of 10 or more P wave arrival times, (5) readings of 5 or more S wave arrival times, and (6) $M = 2.0$ or larger.

Data set 2.

We selected 37 seismographic stations near the aftershock area (Fig. 5b), and read the arrival times of P and S waves from 83 aftershocks with $M = 3.5$ or larger. For each earthquake we picked up both P and S waves at 14 stations without fail: HTU, AKK, NMR, AKSI, NKSB, RAUS, HNKH, BKEH, SCSH, BKWH, NSTH, STSH, TREH, and STNH, and only P wave at 23 stations without fail: NIT, TES, RUS, URH, ASYR, CHRI, JTKR, SCNH, TRSH, TRWH, ANSH, SYSH, ANNH, SNNH, KMZH, BHRH, HBTH, MMBH, RKBH, AYWH, SRMH, OKEH, and RBSH. The seismographic stations included in Hi-net (the high-sensitivity seismographic network) have a station code with four characters ending with “H”. The Hi-net is maintained by the National Research Institute for Earth Science and Disaster Prevention (NIED). Since the arrival times are read from the 37 seismic stations in the fixed configuration, the relative position of hypocenter is expected to be more accurate than that from Data set 1.

2.2.2.2. Relocation of Hypocenters

Since the crust and the upper mantle beneath the Hokkaido Island have very complicated geological structures (e.g., Miyamachi et al., 1994; Moriya et al., 1998), it is not appropriate to use a simple one-dimensional layered velocity structure for the hypocenter calculation. Katsumata et al. (2002) determined three-dimensional (3-D) P and S wave velocity structures in and around the Hokkaido Island by applying a tomographic method developed by Zhao et al. (1992) to arrival time data from shallow and intermediate-depth earthquakes. In this study we assumed this 3-D velocity structure, and relocated the aftershocks included in Data sets 1 and 2. We used a hypocenter calculation method developed by Zhao et al. (1992).

2.2.2.3. Location Errors

We carried out a numerical simulation in order to estimate robustness and a relative error for the hypocenter relocation using Data set 2. The numerical simulation is a so-called bootstrap method. For an earthquake, we selected 37 seismographic stations randomly among the 37 stations described in the section III.1 with allowing to select the same station many times, and calculated a hypocenter. We repeated this procedure one

hundred times. Then the robustness of hypocenter location was estimated by how the resulting hypocenters moved from the original location. We define an error as the standard deviation of one hundred resulting hypocenters. The errors were approximately 1.5 km and 2.0 km for the East-West and North-South directions, respectively, and became larger slightly as a function of distance from the coast. This feature is seen more clearly in the depth direction. The error was constant to be approximately 1.2 km nearer than 30 km from the coast, and became larger than 2.0 km at distance farther than 40 km.

2.2.2.4. Results

Data set 1.

We relocated 582 aftershocks with $M = 2.0$ or larger between 29 November 2004 and 29 January 2005 using Data set 1. From the calculated aftershock locations, we found that most of the aftershocks occurred within the rectangular area with 50 km in the East-West direction and 30 km in the North-South direction (Fig. 6). The outstanding feature is that the aftershocks are located in a cluster like a ring surrounding the main shock on 29 November. On a vertical cross section hypocenters are distributed between 35 and 55 km in depth and the depth appears to become deeper toward the landside. However we are not able to identify a fault plane clearly from the cross section.

The main shock on 29 November was followed by the two large aftershocks. We found that the focal areas ruptured by the three events did not overlap with each other (Fig. 7). The focal areas ruptured by the aftershocks on 6 December and on 18 January were located on the southeastern and the southwestern boundaries of the focal area ruptured by the main shock, respectively.

The background seismicity between 1 January 2002 and 29 November 2004 was active in some earthquake clusters in the focal area. We identified three active clusters centered on (42.8°N, 145.0°E), (42.8°N, 145.3°E), and (42.9°N, 145.4°E), and found that lots of the aftershocks occurred in the three active clusters (Fig. 8).

Data set 2.

We were not able to identify the fault plane clearly on the vertical cross section based on the relocated aftershocks using Data set 1. To obtain more accurate image we relocated 83 aftershocks with $M = 3.5$ or larger between 29 November 2004 and 29 January 2005 using Data set 2. The aftershock distribution is generally same as the results obtained by Data set 1 (Fig. 9). The errors defined in the section III.3 were presented on Fig. 9c-e. On the vertical cross section, the hypocenters are located on a plane dipping 22° toward the landside whose orientation agrees closely with that of the northwest-dipping nodal plane of the focal mechanism. Moreover, the aftershocks

occurred on the upper plane of the double seismic zone presented by Katsumata et al. (2003) (Fig. 10).

2.2.3. Source Process and Aftershock Distribution

Comparing with the source process of the main shock and the aftershock distribution, we found that the aftershocks outlined the asperity ruptured by the main shock (Fig. 11). Yagi et al. (1999) reported that aftershocks of the Hyuga-nada earthquake in 1996 occurred in the area not ruptured by the main shock, and they suggested that in the aftershock area there were barriers that stopped the rupture extent during the main shock. Taking the similar aftershock distribution into account, our plausible interpretation is that many aftershocks of the Kushiro-Oki earthquake concentrated on the regions that played a role of barriers to dynamic rupture in the main shock. We found the three clusters in the aftershock area with high seismicity, which were very active even before the main shock. This activity is apparently caused by the strong mechanical coupling on the plate boundary, and it is possible to play a role of barriers.

2.3. Tsunami Analysis

2.3.1. Data

A small tsunami was generated by the Kushiro-oki earthquake. The tsunami waveforms were observed at three tide gauge stations, Hanasaki, Kushiro, and Urakawa, along the Pacific coast of Hokkaido. Those three tsunami waveforms were used to study the fault parameters of the earthquake. Those tide gauge records were provided by Japan Meteorological Agency.

2.3.2. Analysis

The tsunami waveforms at tide gauges were numerically computed using the focal mechanism estimated from the seismological analysis (strike=238°, dip=33°, rake=117°). The length and width of the fault are assumed to be 15km X 15km. The fault includes the large slip area estimated from the seismological analysis as shown in Fig.12.

Finite difference computations for the linear long-wave (see Satake, 1995) were carried out on the actual bathymetry. The grid size was basically 20 sec of arc (about 600m), but finer grid (4 sec) were used around the tide gauge stations. The computation was made every 1 s to satisfy a stability condition. The initial condition of tsunami propagation was an ocean bottom deformation, which was computed using the equations of Okada (1985).

2.3.3. Results

The observed and computed tsunami waveforms at three tide gauge stations are

compared in Fig.13. By comparing the observed and computed tsunami waveforms, the slip amount of the fault is estimated as 1.7m. By assuming the rigidity of 6.0×10^{10} N/m², the seismic moment is calculated as 2.3×10^{19} Nm (Mw6.9) which is consistent with the seismological analysis.

2.4. Discussions

2.4.1. Source Process and Aftershock Distribution

Comparing with the source process of the main shock and the aftershock distribution, we found that the aftershocks outlined the asperity ruptured by the main shock (Fig. 11). Yagi et al. (1999) reported that aftershocks of the Hyuga-nada earthquake in 1996 occurred in the area not ruptured by the main shock, and they suggested that in the aftershock area there were barriers that stopped the rupture extent during the main shock. Taking the similar aftershock distribution into account, our plausible interpretation is that many aftershocks of the Kushirro-Oki earthquake concentrated on the regions that played a role of barriers to dynamic rupture in the main shock. We found the three clusters in the aftershock area with high seismicity, which were very active even before the main shock. This activity is apparently caused by the strong mechanical coupling on the plate boundary, and it is possible to play a role of barriers.

2.4.2. Average Stress Drop

We calculated the stress drop, $\Delta\sigma$, averaged on the fault plane from $\Delta\sigma = 2.5M_0/S^{1.5}$, where M_0 and S are the seismic moment and the fault area, respectively. We estimated the fault area ruptured by the main shock on 29 November from the extent of the aftershock zone after one day, resulting that the area is $S = 30 \times 15$ km² (Fig. 11). The total seismic moment was $M_0 = 3.4 \times 10^{19}$ Nm obtained by the seismological analysis. Thus we obtain that the average stress drop was $\Delta\sigma = 8.9$ MPa, that is, 89 bars.

From the statistical point of view the $M7.1$ Kushiro-Oki earthquake on 29 November 2004 was a usual event. Bilek and Lay (1998) found that the average stress drop of the interplate event gets larger as the depth of hypocenter gets deeper in the Japan subduction zone (Fig. 14). According to their analysis, the average stress drop is approximately 100 bars around 50 km in depth. For the Kushiro-Oki earthquake we obtained that the depth of hypocenter is 48 km and the average stress drop is 89 bars, which is very consistent with the results obtained by Bilek and Lay (1998).

2.4.3. Seismic Quiescence Area and the Asperity Ruptured by the 1973 Nemuro-Oki Earthquake

In the Nemuro-Oki area, Katsumata and Kasahara (2004) found that the microearthquake seismicity rate within the Pacific plate decreased 48 %, which started

in June 2000 and has been lasting approximately five years. The seismic quiescence area is defined by a circle centered at (43.4°N, 145.0°E) with a radius of 46 km, which referred to Area 4. Fig. 15 shows that the 2004 Kushiro-Oki earthquake is located between the seismic quiescence area and the asperity ruptured by the 1973 Nemuro-Oki earthquake. These areas do not overlap each other.

Murakami (2005) reported at a regular meeting of the Coordinating Committee for Earthquake Prediction on 21 February 2005 that a slow slip with a velocity of 10 cm/year started in mid 2004 on the plate boundary in Area 4, based on data from GEONET, which is a dense GPS network in Japan.

A qualitative hypothesis to describe what is going on in this region is as follows: (1) an aseismic slow slip started in June 2000 on the plate boundary in Area 4, (2) a shear stress was partly released and the seismicity decreased in Area 4, (3) the aseismic slow slip loaded a shear stress on the focal area of the Kushiro-Oki earthquake, and (4) the Kushiro-Oki earthquake occurred on 29 November 2004.

The aseismic slow slip was possibly very small in displacement at the beginning, and the stress drop was relatively large. This is a reason why the aseismic slow slip was not detected by the GPS network until mid 2004 while the seismicity rate had decreased clearly since 2000. We suppose that the aseismic slow slip was accelerated in mid 2004, and was detected by the GPS network.

2.5. Concluding Remarks

We investigated the source process and the aftershock distribution of the 29 November 2004 Kushiro-Oki earthquake, and found that this event is a large underthrusting earthquake rupturing the plate boundary between the subducting Pacific plate and the overriding North American plate. The main shock was a usual event around 50 km in depth from the points of view including the extent of the aftershock zone and the average stress drop. However, taking the location of the focal area into account, this is an outstanding event, which was located between the region suffering from the five-years-lasting seismic quiescence and the asperity ruptured by the 1973 Nemuro-Oki earthquake. Moreover, an aseismic slow slip has been observed since mid 2004 in the seismic quiescence area.

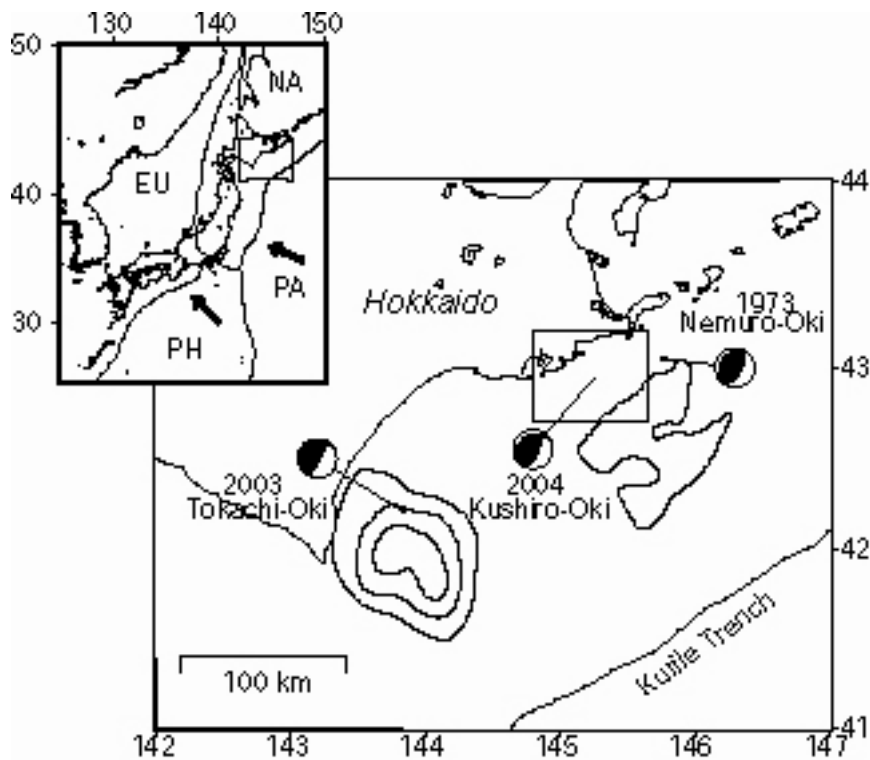


Fig.1. Hokkaido subduction zone. Focal mechanisms are shown for the 2003 Tokachi-Oki earthquake ($M = 8.3$), the 1973 Nemuro-Oki earthquake ($M = 7.4$), and the 2004 Kushiro-Oki earthquake ($M = 7.1$). Asperities are shown in contour every 1 m for the Tokachi-Oki and the Nemuro-Oki earthquakes (Yamanaka and Kikuchi, 2003). A rectangle indicates the area shown in the following figures 6, 7, 8, 9, and 11. Inset shows the area covered by the study area and the plate configuration. PA: Pacific plate, PH: Philippine Sea plate, EU: Eurasian plate, NA: North American plate. Arrows show the direction of plate motion relative to the Eurasian plate.

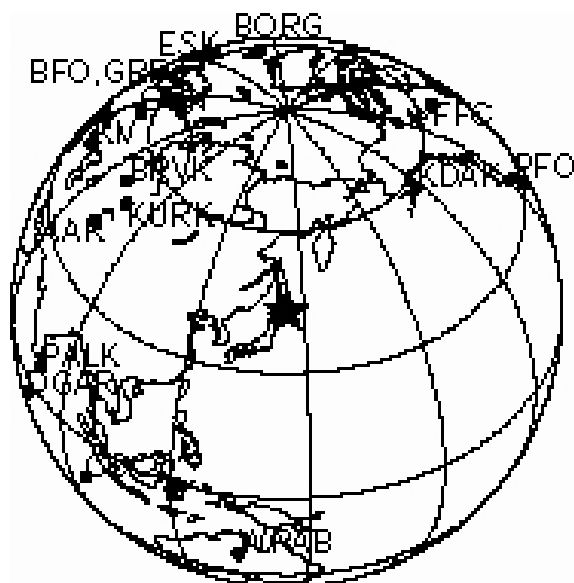


Fig.2. Seismographic stations used for the waveform inversion: FFC, KDAK, PFO, WRAB, COCO, DGAR, PALK, AAK, KURK, BRVK, KIV, OBN, GRFO, BFO, ESK, and BORG.

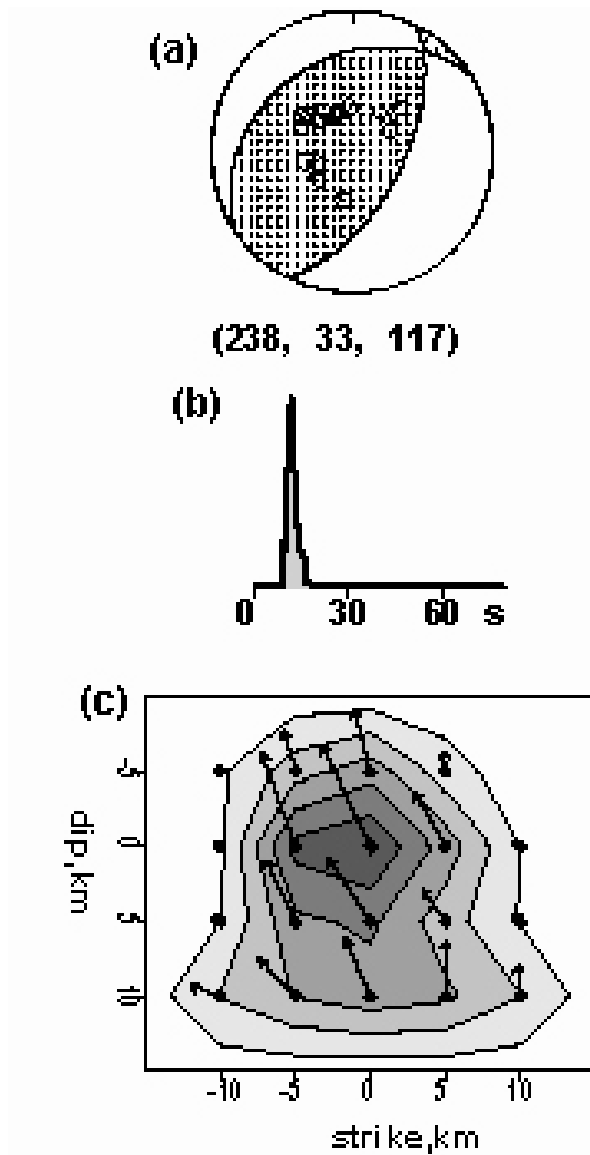


Fig.3. (a) Focal mechanism, (b) source time function of the moment rate, and (c) slip distribution of the 29 November 2004 Kushiro-Oki earthquake. Contours in (c) are drawn from 0.3 to 2.7 m every 0.6 m. Arrows indicate slip vectors of the hanging wall at each grid point. Positive direction in the strike-axis points to the azimuth 238°, and positive direction in the dip-axis points to 33° downward from the horizon.

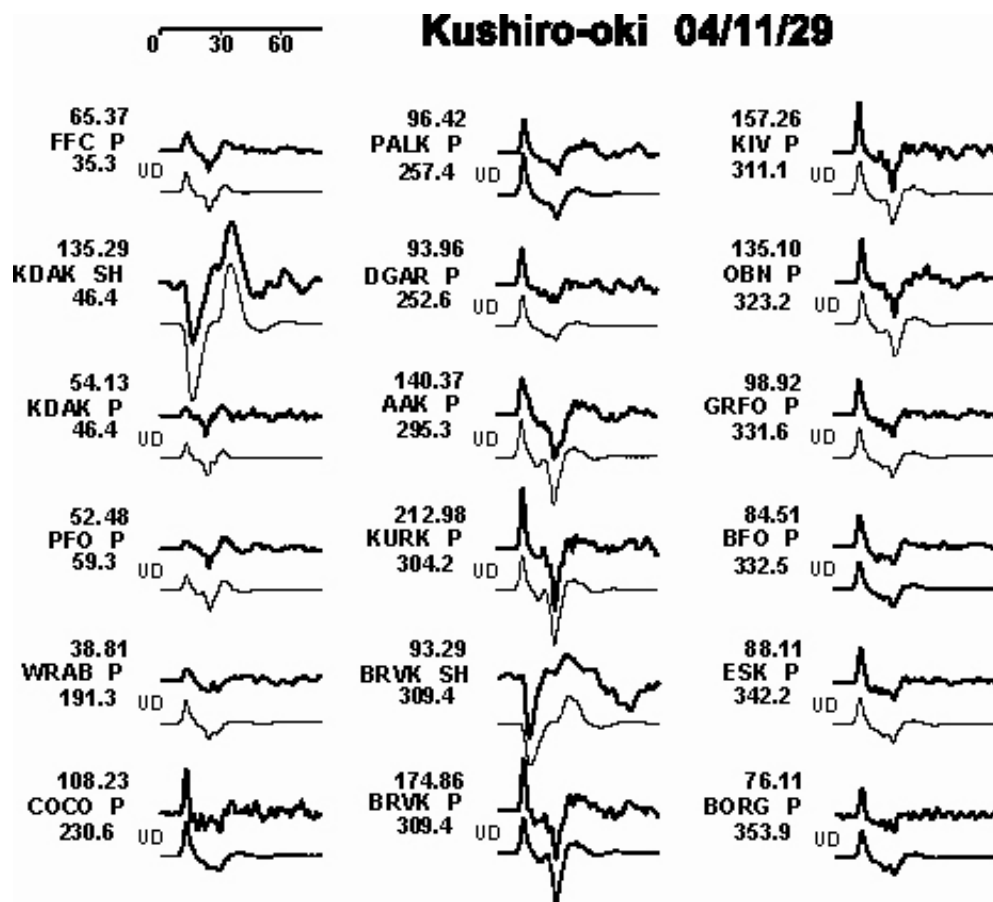


Fig.4. Observed (upper bold lines) and synthetic (lower thin lines) waveforms at each seismic station. The numbers above the station codes are peak-to-peak amplitudes of the observed waveforms in microns, and numbers below are the azimuths of the station from the earthquake.

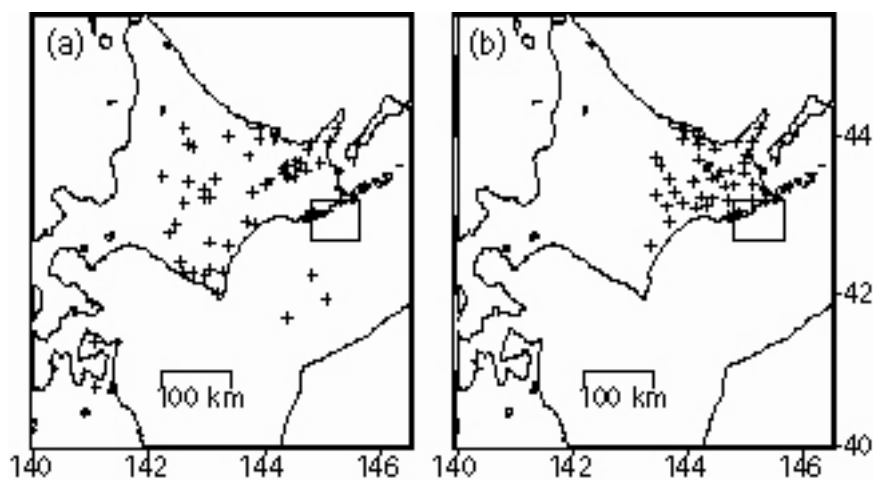


Fig.5. Seismographic stations used for relocating aftershocks, (a) for Data set 1 and (b) for Data set 2. A rectangle indicates the study area shown in figures 6, 7, 8, 9, and 11.

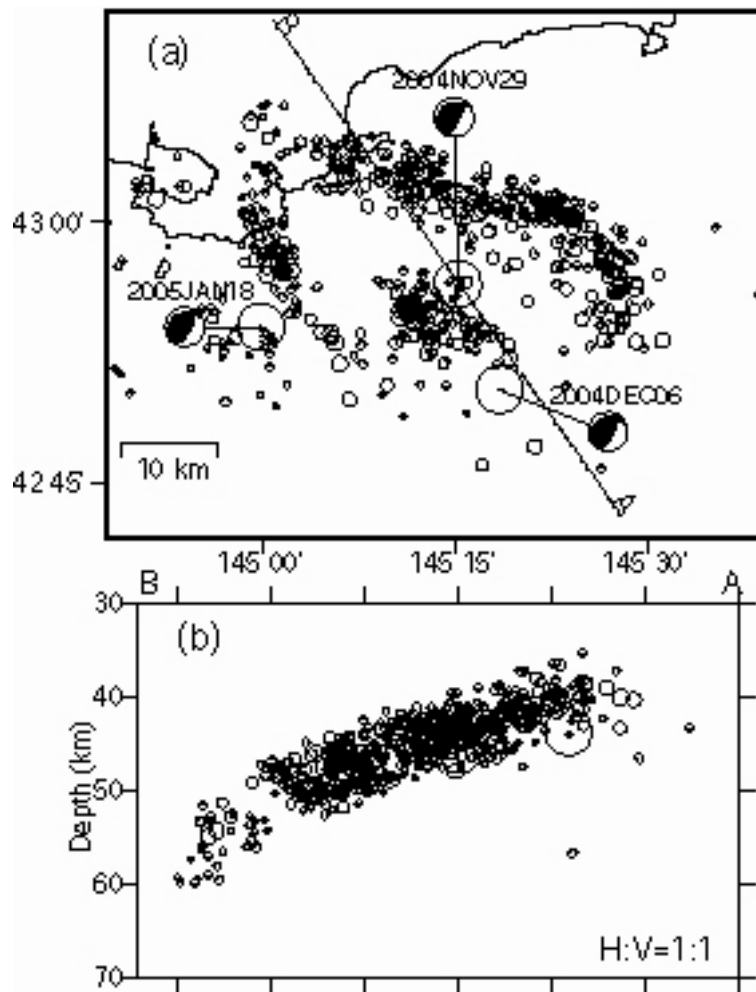


Fig.6. Aftershocks of the 29 November 2005 Kushiro-Oki earthquake relocated by using three-dimensional velocity structure based on Data set 1. The time period is from 29 November 2004 to 29 January 2005, and the magnitude is 2.0 or larger. (a) Map view and (b) vertical cross section along the line A-B in (a). The focal mechanisms were determined by Harvard University, which are equal area projections of the lower hemisphere of the focal sphere.

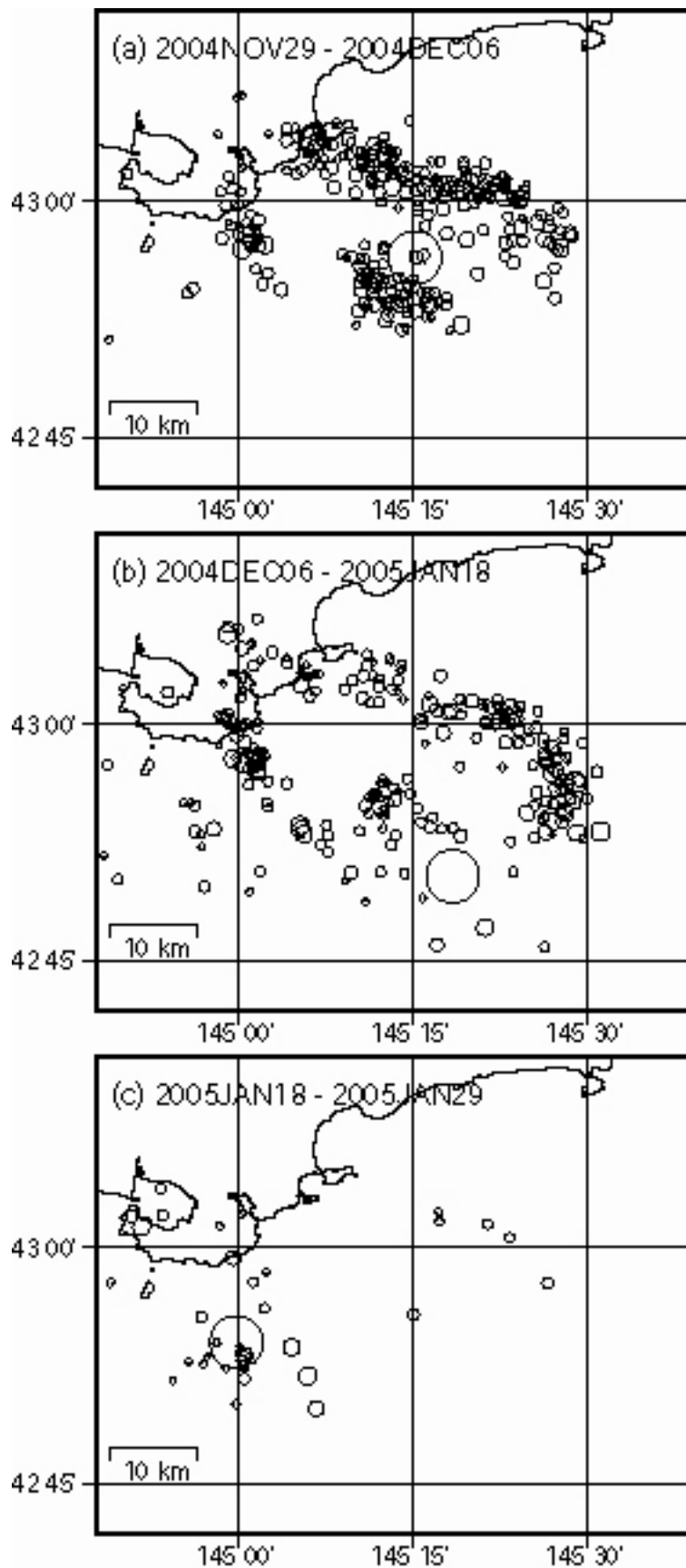


Fig.7. Time slices of the aftershock activity following the 29 November 2005 Kuroshio-Oki earthquake. (a) From the $M = 7.1$ main shock to the occurrence of the $M = 6.9$ aftershock on 6 December 2004, (b) from the $M = 6.9$ aftershock to the occurrence of the $M = 6.4$ aftershock on 18 January 2005, and (c) from the $M = 6.4$ aftershock to 29 January 2005.

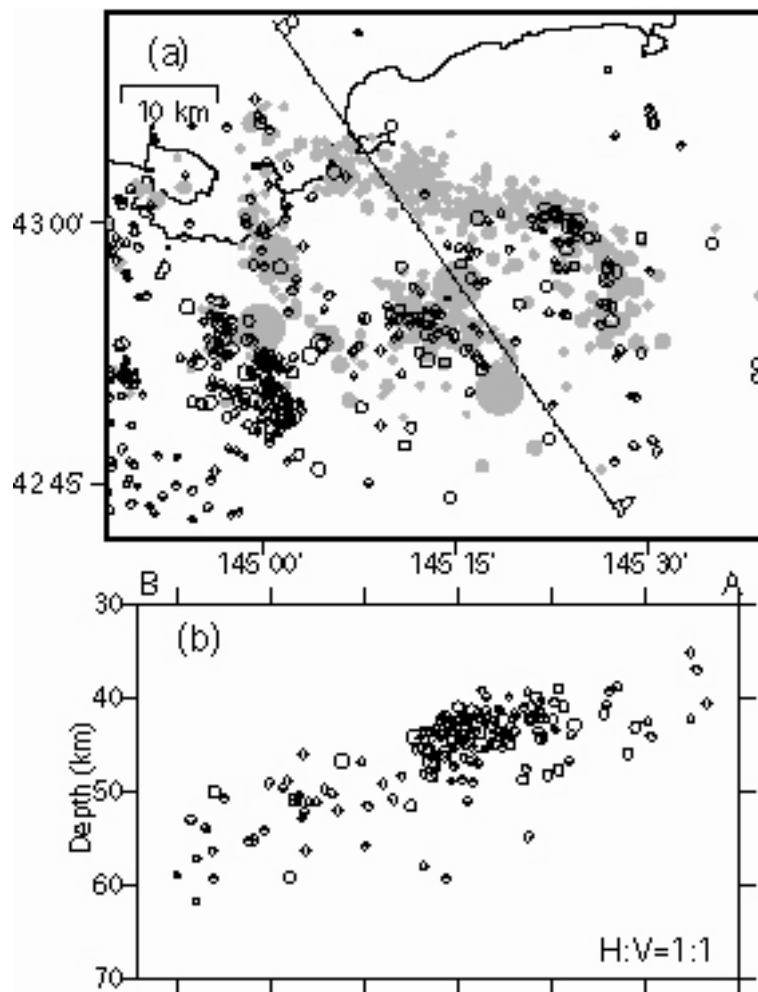


Fig.8. Background seismicity from 1 January 2002 to 28 November 2004 (open circles) and the aftershocks of the 29 November 2004 Kushiro-Oki earthquake (gray circles). (a) Map view and (b) vertical cross section along the line A-B in (a). Note that the aftershocks were not plotted on (b).

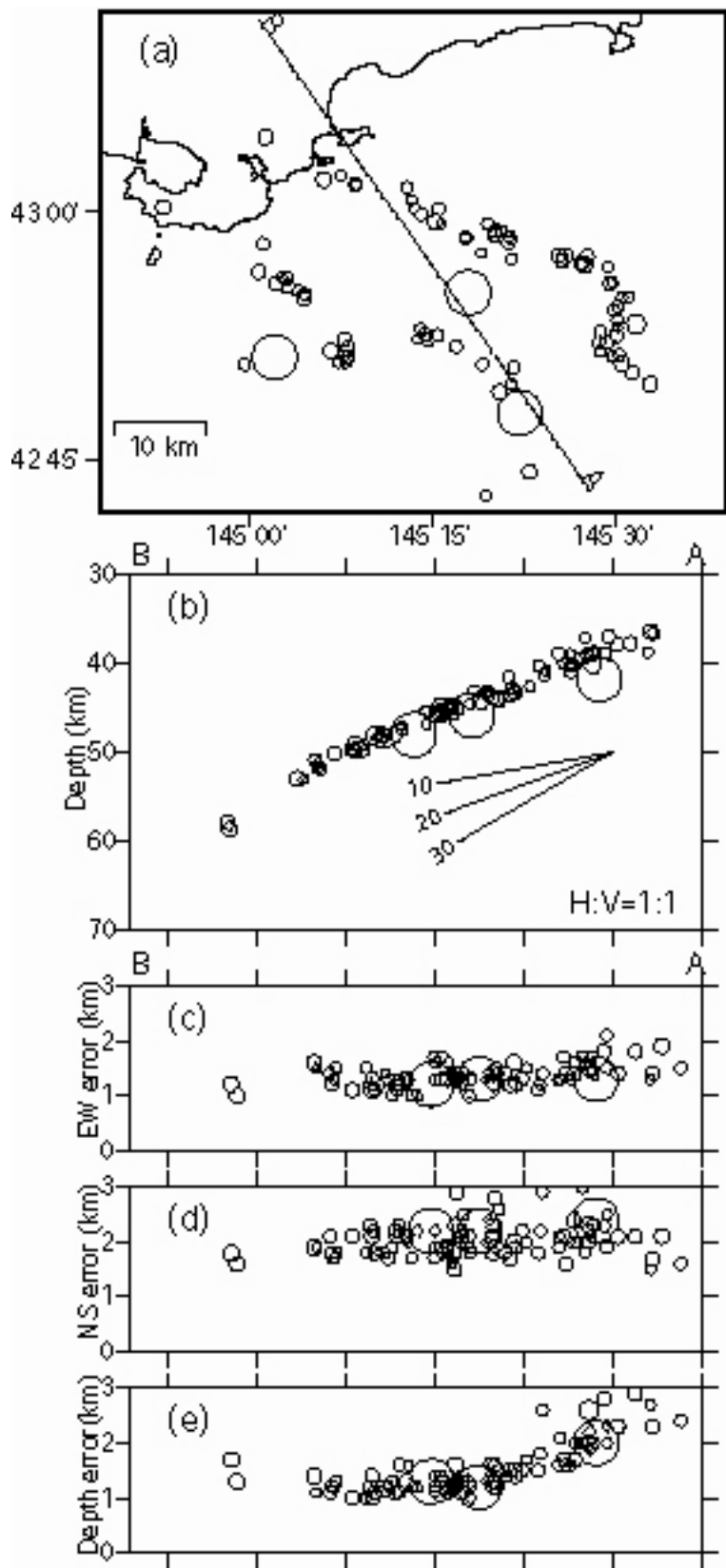


Fig.9. Aftershocks of the 29 November 2005 Koshiro-Oki earthquake relocated by using three-dimensional velocity structure based on Data set 2. The time period is from 29 November 2004 to 29 January 2005, and the magnitude is 3.5 or larger. (a) Map view and (b) vertical cross section along the line A-B in (a). (c)-(e) The location errors defined in the section 3.3 in this paper.

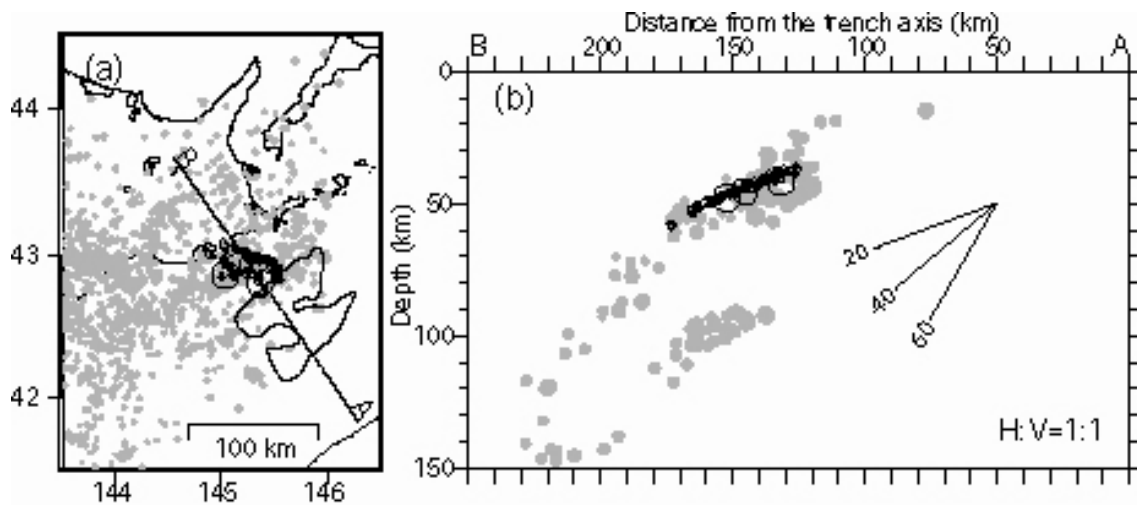


Fig.10. Regional background seismicity from July 1999 to July 2001 presented by Katsumata et al. (2003) (gray circles), and the aftershocks of the 29 November 2004 Kushiro-Oki earthquake (open circles), which were relocated using Data set 2. (a) Map view with a contour of 1 m indicating the asperity ruptured by the 1973 Nemuro-Oki earthquake determined by Yamanaka and Kikuchi (2002), (b) vertical cross section along the line A-B in (a).

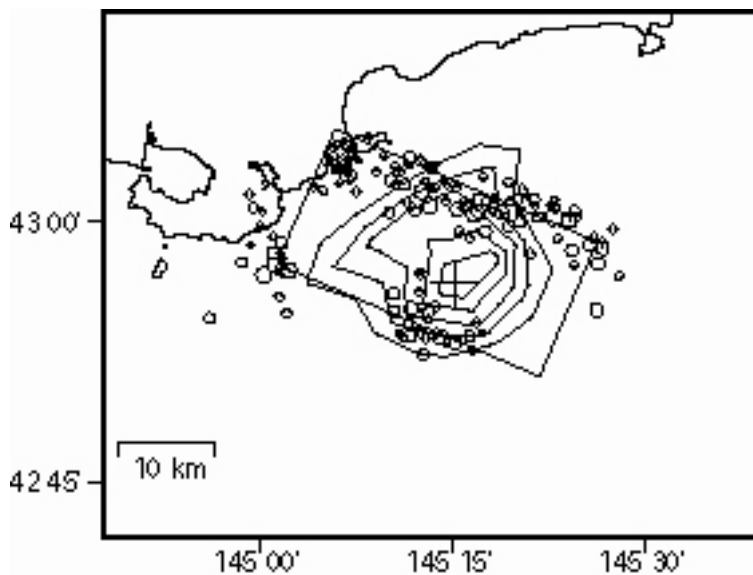


Fig.11. Aftershock area of the 29 November 2004 Kushiro-Oki earthquake after one-day and the slip distribution. The cross and open circles indicate the epicenter of the main shock and aftershocks, respectively. A rectangle represents the area ruptured by the main shock, which was used for calculating the stress drop. Contours are drawn from 0.3 to 2.7 m every 0.6 m.

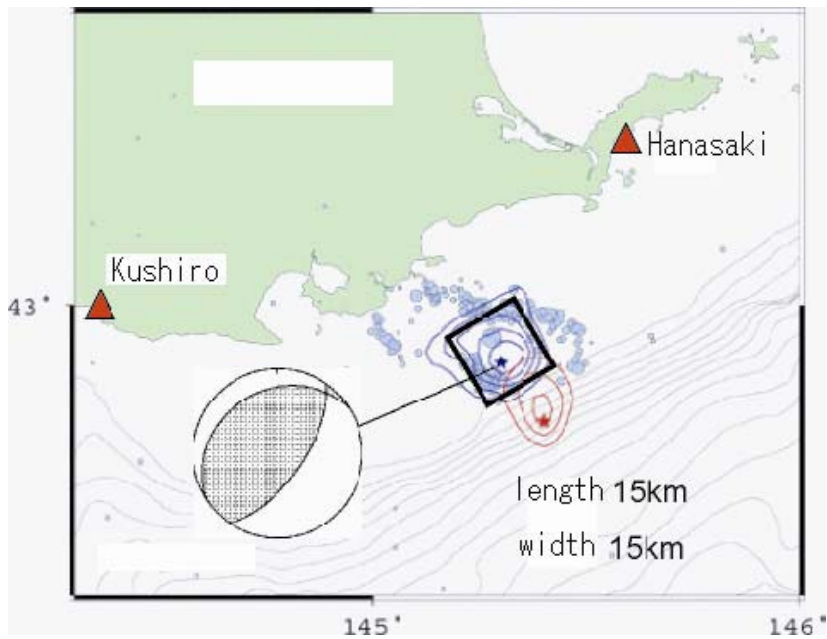


Fig.12. The mechanism and the fault model of the 2004 Kushi-Oki earthquake. The triangles represent the location of tide gauges.

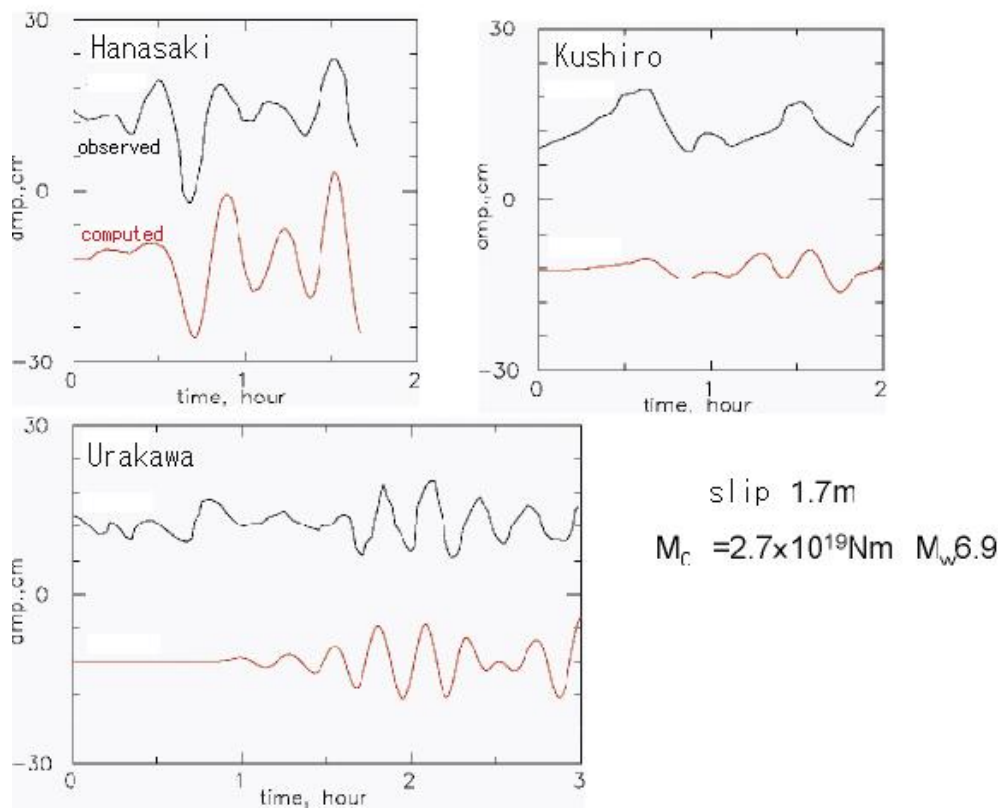


Fig.13. Comparison between observed and computed tsunami waveforms for the 2004 Kushi-Oki earthquake.

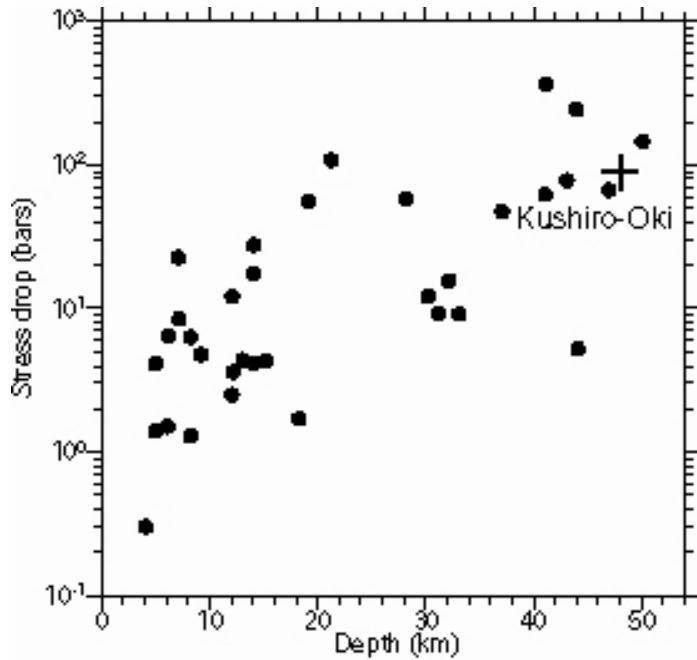


Fig.14. Stress drop as a function of depth of hypocenter in the Japan trench after Bilek and Lay (1998) (closed circles). A cross indicates the stress drop and the depth for the 29 November 2004 Kushiro-Oki earthquake determined in this study.

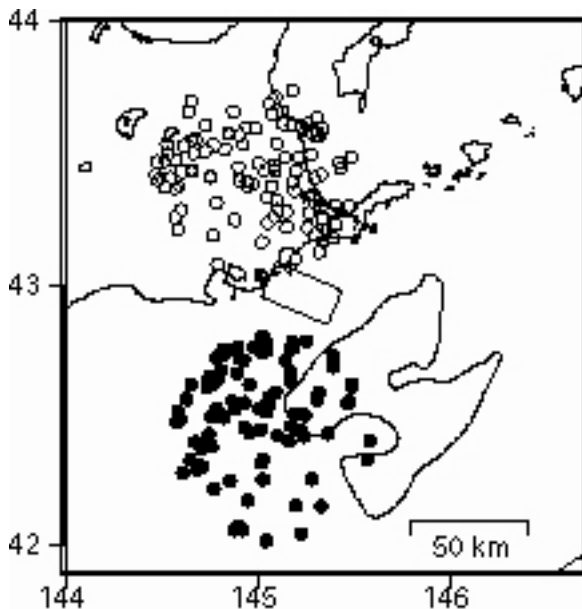


Fig.15. Aftershock area, asperity, and change in seismicity rate. Earthquakes within the Pacific plate has been suffered from the seismic quiescence (open circles) and the seismic activation (closed circles) since May 2000 (Katsumata and Kasahara, 2004). A rectangle indicates the area ruptured by the main shock on 29 November 2004, which is same as that in Fig. 11. A contour of 1 m represents the asperity ruptured by the 1973

Nemuro-Oki earthquake determined by Yamanaka and Kikuchi (2002).

3. A future Nemuro-Oki earthquake

3.1. Introduction

A future great Nemuro-oki earthquake has been expected by the Headquarters for Earthquake Research Promotion in Japan (HERP) with the high probability of the occurrence during 30 years from October 1, 2003, 20-30%. It is important to discuss the source process of the future Nemuro-oki earthquake.

Previously, the great earthquakes occurred off Nemuro in 1973 and 1894. The source process of the 1973 Numuro-Oki earthquake was previously studied by many researchers. The magnitude of the earthquake was estimated to be 7.4 by JMA. The total seismic moment was 6.7×10^{20} Nm ($M_w = 7.8$) and the average fault slip was 1.6 m determined by Shimazaki (1974) using surface-wave data. Tada (1974) estimated that the average fault slip was 1.0 m using geodetic data. However, the source process of the 1894 earthquake was not studied well because no seismograph or geodetic data are available for this event. The tsunami generated by the 1894 Nemuro-oki earthquake was observed at the tide gauge station in Ayukawa. This tsunami waveform is the only one instrumental record for this earthquake. In this research, we study the source process of the 1973 and 1894 earthquake using the tsunami waveform at the tide gauge in Ayukawa to discuss the future Nemuro-oki earthquake.

Also, the most recent seismic activity in the source region of the future Nemuro-oki earthquake is studied using the ocean bottom seismic network deployed after the 2004 Kushiro-oki earthquake.

3.2. The 1973 and 1894 Nemuro-Oki earthquake

3.2.1. Data and Method

The tsunami waveforms from both the 1973 and 1894 Nemuro-Oki earthquakes were observed at the tide gauge at Ayukawa shown in Fig.16. The observed tsunami waveform of the 1894 Nemuro-Oki earthquake is very different from that of the 1973 Nemuro-Oki earthquake. Fortunately, the bathymetry near Ayukawa has not been changed much since 1894, so the difference between two tsunami waveforms should be related to the different source processes between two earthquakes. However, the absolute time of the record in 1894 does not have enough accuracy for this analysis, so we shifted the time of record by comparing the observed and computed waveforms.

We numerically computed the tsunami waveform for the 1973 earthquake by assuming the fault model consistent with the previous studies, the length of 80km, the

width of 80km, strike of 240°, dip=14°, rake=111° (Fig.16). The tsunami for the 1894 earthquake was computed using the various fault length and width to find the fault model which could explain the observed 1894 tsunami waveform. The focal mechanism was assumed to be the same as that of the 1973 earthquake.

Finite difference computations for the linear long-wave (see Satake, 1995) were carried out on the actual bathymetry. The grid size was basically 20 sec of arc (about 600m), but finer grid (4 sec) were used around the tide gauge stations. The computation was made every 1 s to satisfy a stability condition. The initial condition of tsunami propagation was an ocean bottom deformation, which was computed using the equations of Okada (1985).

3.2.2. Results

For the 1973 Nemuro-Oki earthquake, the slip amount of the 1973 was estimated to be 2m in order to explain the observed tsunami waveforms at Ayukawa. A blue rectangle in Fig.17 shows the location of the fault model. In Fig.16, the observed tsunami waveform at Ayukawa was well explained by the computed one. The seismic moment was calculated to be 5.1×10^{20} Nm (Mw 7.8).

For the 1894 Nemuro-Oki earthquake, the length of the fault should be 200km, much longer than the length of the fault of the 1973 earthquake. The location of the fault is shown in Fig.17. The width of the fault is found to be 100km, and the slip amount is estimated to be 2.4m by comparing the observed and computed tsunami waveforms (Fig.16). The seismic moment was calculated to be 19.2×10^{20} Nm (Mw 8.2).

3.3. The Seismic Activity Using Ocean Bottom Seismic Network

3.3.1. Data

Ten ocean bottom seismometers were installed from April 1 to May 31, 2005 and made a network near the source region of the future Nemuro-Oki earthquake (Fig.18). The hypocenters of the earthquakes occurred during the installation period were determined.

3.3.2. Results

The results of the seismic activity in the source region determined by the ocean bottom seismic network was shown in Fig.18. The seismic activity beneath the seismic network, the red dashed circle in Fig.18, is generally very low, except beneath the red solid circle region in Fig.18.

3.4. Discussions

The future Nemuro-Oki earthquake can be larger than the 1973 Nemuro-Oki

earthquake because the 1894 Nemuro-Oki earthquake has a fault length of about 200km, much larger than the 1973 Nemuro-Oki earthquake. Also the source area of the 2003 Tokachi-Oki earthquake was smaller than the 1952 Tokachi-Oki earthquake. The seismic activity in the source region of the future Nemuro-Oki earthquake is very low now. This may suggest that the coupling at the plate interface in the source region is strong and the occurrence of the future Nemuro-Oki earthquake is confirmed in the region.

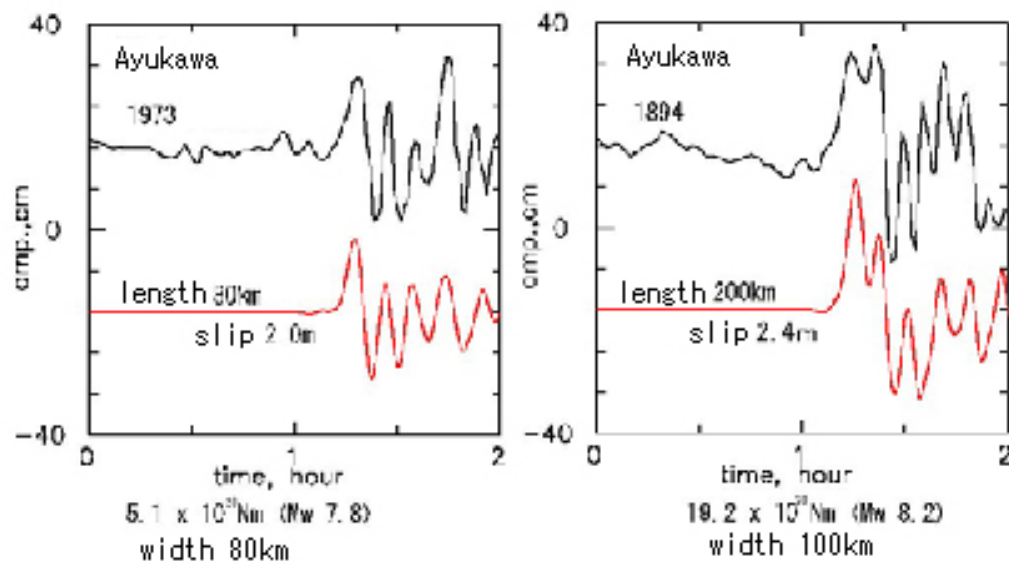


Fig.16 Comparison of the observed (black) and computed (red) tsunami waveforms at Ayukawa for the 1973 Nemuro-Oki (left) and 1894 Nemuro-Oki (right) earthquakes.

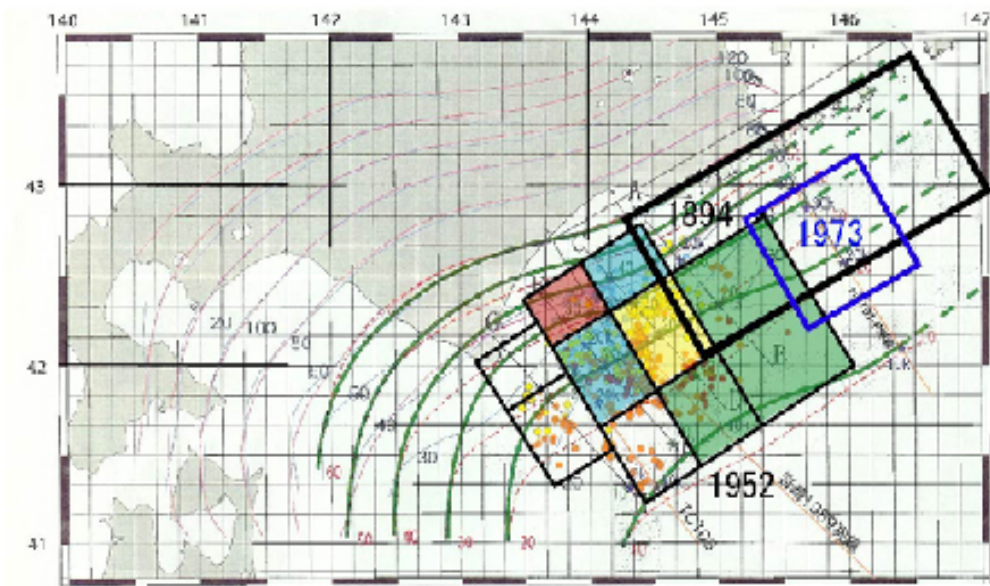


Fig.17. The fault models for the 1973 Nemuro-Oki and 1894 Nemuro-Oki earthquakes. The slip distribution of the 1952 Tokachi-oki earthquake estimated by Hirata et al. (2003) is also shown.

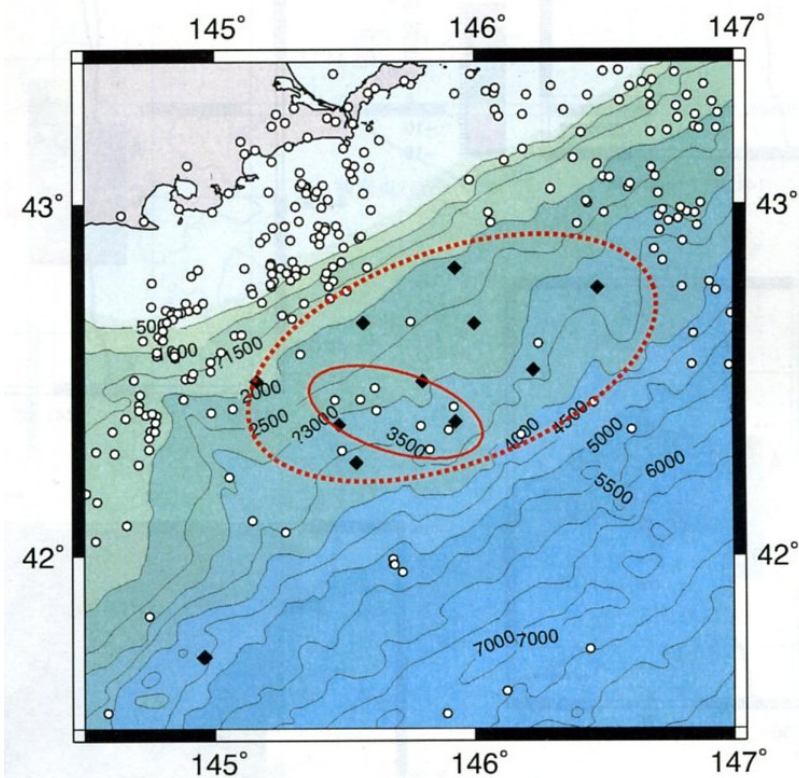


Fig.18. The seismicity near the source region of the future Nemuro-Oki earthquake determined by the ocean bottom seismic network. Open circles are the epicenter of the earthquake. Solid diamonds show the location of ocean bottom seismometers.

References

- Bilek, S. and T. Lay, 1998. Variation of interplate fault zone properties with depth in the Japan subduction zone, *Science*, **281**, 1175-1178.
- DeMet, C., R. Gordon, F. Argus, and S. Stein, 1994. Effect of recent revisions to the geomagnetic reversal time scale on estimates of current plate motions, *Geophys. Res. Lett.*, **21**, 2191-2194.
- Hirata, K., E. L. Geist, K. Satake, Y. Tanioka, and S. Yamaki, 2003. Slip distribution of the 1952 Tokachi-oki earthquake (M8.1) along the Kuril Trench deduced from tsunami waveform inversion, *J. Geophys. Res.*, **108(B4)**, 2196, doi:10.1029/2002JB001976.
- Iwasaki, T., H. Shiobara, A. Nishizawa, T. Kanazawa, K. Suyehiro, N. Hirata, T. Urabe, and H. Shimamura, 1989. A detailed subduction structure in the Kurile trench deduced from ocean bottom seismographic refraction studies, *Tectonophysics*, **165**, 315-336.
- Katsumata, K., M. Ichiyangi, M. Miwa, M. Kasahara, and H. Miyamachi, 1995. Aftershock distribution of the October 4, 1994 Mw 8.3 Kurile Islands earthquake determined by a local seismic network in Hokkaido, Japan, *Geophys. Res. Lett.*, **22**, 1321-1324.
- Katsumata, K., N. Wada, and M. Kasahara, 2002. Three-dimensional *P* and *S* wave velocity structures beneath the Hokkaido corner, Japan-Kurile arc-arc junction, *Abstracts of the Fall Meeting of the Seismological Society of Japan*, P180 (in Japanese).
- Katsumata, K., N. Wada, and M. Kasahara, 2003. Newly imaged shape of the deep seismic zone within the subducting Pacific plate beneath the Hokkaido corner, Japan-Kurile arc-arc junction, *J. Geophys. Res.*, **108(B12)**, 2565, doi:10.1029/2002JB002175.
- Katsumata, K. and M. Kasahara, 2004. Precursory seismic quiescence prior to the 2003 Tokachi-Oki earthquake and the present seismicity in the neighboring area, *Abstracts of the fall meeting of the Seismological Society of Japan*, A48 (in Japanese).
- Kikuchi, M. and H. Kanamori, 1991. Inversion of complex body waves – III, *Bull. Seism. Soc. Am.*, **81**, 2335-2350.
- Kikuchi, M. and H. Kanamori, 2003. Note on Teleseismic Body-Wave Inversion Program, <http://www.eri.u-tokyo.ac.jp/ETAL/KIKUCHI/>.
- Miyamachi, H., M. Kasahara, S. Suzuki, K. Tanaka, and A. Hasegawa, 1994. Seismic velocity structure in the crust and upper mantle beneath northern Japan, *J. Phys.*

- Earth*, **42**, 269-301.
- Moriya, T., H. Okada, T. Matsushima, S. Asano, T. Yoshii, and A. Ikami, 1998. Collision structure in the upper crust beneath the southwestern foot of the Hidaka Mountains, Hokkaido, Japan as derived from explosion seismic observations, *Tectonophysics*, **290**, 181-196.
- Murakami, M., 2005. Crustal deformation in the eastern Hokkaido after the 2003 Tokachi-Oki earthquake, A report presented at a regular meeting of the Coordinating Committee for Earthquake Prediction on 21 February 2005.
- Okada, Y., 1985, Surface deformation due to shear and tensile faults in a half-space, *Bull. Seismol. Soc. Am.*, **75**, 1135-1154.
- Satake, K., 1995, Linear and nonlinear computations for the 1992 Nicaragua earthquake tsunami, *Pure Appl. Geophys.*, **144**, 455-470.
- Shimazaki, K. 1974. Nemuro-Oki earthquake of June 17, 1973: A lithospheric rebound at the upper half of the interface, *Phys. Earth Planet. Inter.* **9**, 314-327.
- Tada, T., 1974. Fault model and crustal movement of the 1973 Nemuro-Oki earthquake, *J. Seism. Soc. Japan (Zisin)*, **27**, 120-128 (in Japanese).
- Wessel, P., and W. H. F. Smith, 1991. Free software helps map and display data, *Eos Trans. AGU*, **72**, 445-446.
- Yagi, Y., M. Kikuchi, and S. Yoshida, 1999. Comparison of the coseismic rupture with the aftershock distribution in the Hyuga-nada earthquakes of 1996, *Geophys. Res. Lett.*, **26(20)**, 3161-3164.
- Yamanaka, Y. and M. Kikuchi, 2002. Asperity map along the subduction zone in Hokkaido region inferred from historical seismograms, *Abstracts of the fall meeting of the Seismological Society of Japan*, B52 (in Japanese).
- Yamanaka, Y. and M. Kikuchi, 2003. Source process of the recurrent Tokachi-oki earthquake on September 26, 2003, inferred from teleseismic body waves, *Earth Planets Space*, **55(12)**, e21-e24.
- Zhao, D., A. Hasegawa, and S. Horiuchi, 1992. Tomographic imaging of P and S wave velocity structure beneath northeastern Japan, *J. Geophys. Res.*, **97**, 19909-19928.

Published Paper

Katsumata, K., and Y. Yamanaka, The 29 November 2004 *M*7.1 Kushiro-Oki earthquake: An event between the on-going seismic quiescence area and the asperity ruptured by the 1973 Nemuro-Oki earthquake, *Geophysical Bulletin of Hokkaido University*, in press.